Monitoring the development of microcracks in reinforced concrete caused by sustained loading and chloride induced corrosion

Junjie Wang, P.A. Muhammed Basheer, Sreejith V. Nanukuttan

School of Planning, Architecture and Civil Engineering, Queen's University Belfast, Northern Ireland, UK.

Yun Bai

Department of Civil, Environmental & Geomatic Engineering, University College London, England, UK.

ABSTRACT: Chloride-induced corrosion of steel in reinforced concrete structures is one of the main problems affecting their durability and it has been studied for decades, but most of them have focused on concrete without cracking or not subjected to any structural load. In fact, concrete structures are subjected to various types of loads, which lead to cracking when the tensile stress in concrete exceeds its tensile strength. Cracking could increase transport properties of concrete and accelerate the ingress of harmful substances (Cl^-, O_2, H_2O, CO_2). This could initiate and accelerate different types of deterioration processes in concrete, including corrosion of steel reinforcement. The expansive products generated by the deterioration processes themselves can initiate cracking. The success of concrete patch repairs can also influence microcracking at the interface as well as the patch repair itself. Therefore, monitoring the development of microcracking in reinforced concrete members is extremely useful to assess the defects and deterioration in concrete structures. In this paper, concrete beams made using 4 different mixes were subjected to three levels of sustained lateral loading (0%, 50% and 100% of the load that can induce a crack with width of 0.1 mm on the tension surface of beams - $F_{0.1}$) and weekly cycles of wetting (1 day)/drying (6 days) with chloride solution. The development of microcracking on the surface of concrete was monitored using the Autoclam Permeability System at every two weeks for 60 weeks. The ultrasonic pulse velocity of the concrete was also measured along the beam by using the indirect method during the test period. The results indicated that the Autoclam Permeability System was able to detect the development of microcracks caused by both sustained loading and chloride induced corrosion of steel in concrete. However, this was not the case with the ultrasonic method used in the work (indirect method applied along the beam); it was sensitive to microcracking caused by sustained loading but not due to corrosion.

1 INTRODUCTION

Presence of microcracks can accelerate the chloride ingress into the concrete (Wang et al., 2013b, Wang et al., 2011), air permeability and sorptivity of concrete (Wang et al., 2013a), and could accelerate the deterioration process of reinforced concrete structures. Detecting and monitoring cracks, especially the microcracks, is very important for the repair of reinforced concrete structures. Ultrasonic method can be used to detect microcracking caused by sustained loading (Wang et al., 2013a, 2013b) and freezing/thawing cycles (Jacobsen et al., 1996). In the work reported by Wang et al. (Wang et al., 2013b), ultrasonic pulse velocity measurements using different transducer orientations were related to cracking caused by sustained loading. Autoclam tests were also found to be able to detect the microcracking caused by loading (Wang et al., 2013a). However, the effectiveness of these two methods for detecting and monitoring microcracks caused by corrosion of steel in concrete has rarely been studied. In this work, the ultrasonic pulse velocity measurements and Autoclam permeability tests were used to detect and monitor the development of cracks caused by the combined effects of sustained loading and corrosion of steel in concrete, and the results are compared.

2 EXPERIMENTAL PROGRAMME

Class 42.5N CEM I conforming to BS EN 197-1:2011 was used in the work. The coarse aggregate used was crushed and well graded basalt of size 5-20 mm (size 5-10 mm and 10-20mm mixed in the ratio 1:2) and the fine aggregate was natural medium graded sand. Both aggregates were oven-dried at 100 (± 5)℃ for 24 hours to remove the initial moisture content, but the mix water content was adjusted by adding extra water to compensate for the aggregate absorption so as to ensure that the aggregates were in saturated surface dry condition at the time of mixing. Ground granulated blast-furnace (GGBS) complying with BS EN 6699: 1992 was used to replace CEM I by 35% in two mixes. Two different water-binder ratios (w/b), 0.45 and 0.65, were considered. The proportions for each mix are reported in Table 1.

Table 1 Concrete mix proportions (kg/m^3)

Mix ID	0.45-CEM I	0.45-35%GGBS	0.65-CEMI	0.65-35%GGBS
CEMI	360	234	300	105
GGBS	—	126	—	195
Water	162	162	195	195
Superplasticiser	0.47	0.42	—	—
Sand	776	772	761	754
5-10 mm	384	382	376	373
10-20 mm	780	776	764	758

Six beams (1200 × 250 × 200 mm in size) and six 100 mm size cubes were cast for each mix. The reinforcement drawing of the beams is shown in Figure 1. The required quantities of the mix constituents were batched by mass and then mixed using a pan mixer in accordance with BS 1881:125: 1986. The workability of the mixes was determined using the slump test and the slump of each mix is reported in Table 2. A vibrating table was used to compact concrete in the cubes and a poker vibrator was used to compact concrete in the beams. The top surface of the specimens was then finished with a trowel and a thick black polythene sheet was used to cover the surface. The cubes were demoulded after 24 hours and then placed in water bath at 20 (± 1)℃ for the next 3 days, and then wrapped in wet hessian and thick polythene sheet. The beams were demoulded after 7 days and then wrapped in wet hessian and the thick polythene sheet. All specimens were then placed in a constant temperature room at 20 (± 1)℃. The compressive strength test was conducted on three cubes per mix at the age of 28 and 56 days and the results are reported in Table 2.

At the age of 56 days, two concrete beams of each mix were subjected to three loading levels (0%, 50% and 100% of the load that can induce crack with a width of 0.1 mm on the tension surface of the beam - $F_{0.1}$), as shown in Figures 1 and 2. The tension face of all beams was then subjected to weekly cycles of wetting (for 1 day) and drying (for 6 days) with chloride solution (10% NaCl by weight) for 60 weeks. The ponding setup is shown in Figure 3. All faces except the exposure faces were sealed with epoxy paint to ensure ingress of chloride ions through only the tension faces. The intensity of load was kept constant during the test period by topping up the level, if needed, at every 20 weeks. The experimental stages are illustrated in Figure 4. Ultrasonic pulse velocity (UPV), Autoclam air permeability and then water absorption tests were conducted on the exposure surface of beams every 2 weeks before wetting with the chloride solution.

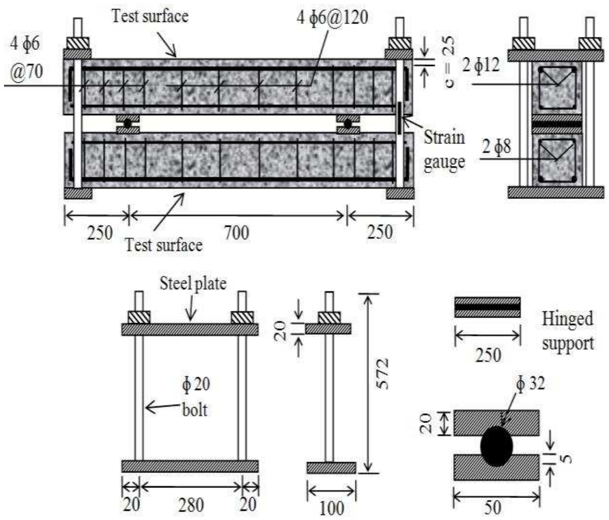

Figure 1. Schematic setup and reinforcement drawing

Table 2 Physical properties of concrete

Mix ID	0.45-CEMI	0.45-35%GGBS	0.65-CEMI	0.65-35%GGBS
Slump (mm)	120.0	95.0	95.0	100.0
f_c* 28d (MPa)	58.0	50.7	37.8	35.1
f_c 56d (MPa)	59.5	56.7	38.7	48.9


Figure 2. Test beams under sustained loading

Ultrasonic pulse velocity (UPV) test, with an indirect method of testing (Jacobsen et al., 1996), was used to quantify the microcracking, as shown in Equation 1. The change in UPV of concrete compared with the initial UPV of the concrete was described as a damage degree of the concrete surface, θ.

$$\theta = (V_0 - V)/V_0 \qquad \text{(Eq. 1)}$$

where θ is the measured damage degree; V_0 is the UPV of the concrete at the initial state before loading; V is the UPV of the concrete during test period.

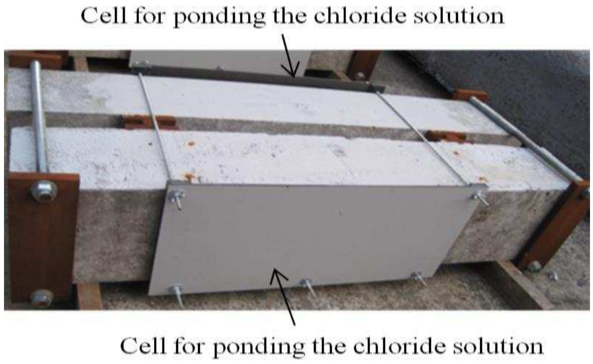

Figure 3. Setup for ponding cells

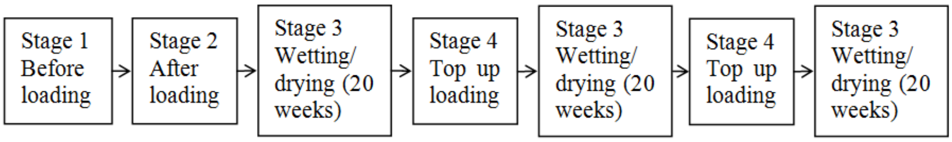

Figure 4 Diagram of test stages

There might be some error in measuring the exact length of the transmission path with the indirect transmission due to a significant contact area between the transducer and the concrete. Therefore, a series of measurements, in accordance with BS EN 12504-4: 2004 was made with the receiver transducers at different distances with fixed increments, as shown in Figure 5. The measurement points were kept to be the same each time. Vaseline petroleum jelly was used as a couplant between the transducer and the concrete surface. The transducers were pressed by hand to exert a constant force against the concrete surface to ensure good acoustic contact. Repeated readings at each location were taken and the minimum transit time was reported. After the test, the test locations were polished with sand paper to remove the jelly from concrete surface.

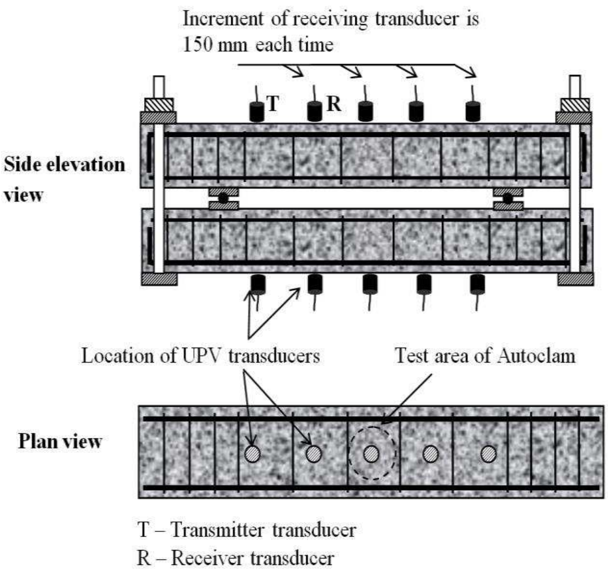

Figure 5. Location of testing points for UPV test and Autoclam test

Note: The testing points and areas were chosen to avoid influence of rebar.

The in situ air permeability and water absorption were then measured using the Autoclam Permeability System (Basheer, 1991), and an air permeability index and a sorptivity index were determined for each of the test condition and the mix. In the air permeability test, compressed air (around 500 mbar) in the Autoclam was allowed to dissipate into the concrete and the pressure of air in the Autoclam was recorded every minute. A graph of natural logarithm of pressure monitored in the test from 5th minute to 15th minute was plotted on the Y-axis against the corresponding time in minutes on the X-axis. The absolute value of the slope of the straight line is reported as air permeability index (API) with units Ln(Pressure)/min. If a test did not last for 15 minutes, the available data were used to calculate the air permeability index.

The water absorption (sorptivity) test was conducted at least 60 minutes after the air permeability test at the same location in order to ensure that the pore pressure due to the air permeability test had dissipated. The water inside the chamber of Autoclam was allowed to ingress into the concrete by absorption through the contact area, and the volume of the water leaving the chamber was recorded every minute. The quantity of water inflow in m^3 between the 5th and 15th minutes was plotted on the Y-axis against square root of the corresponding time in minutes on the X-axis, and the slope of the straight line graph was reported as the sorptivity index (SI), with units $m^3/min^{0.5}$. The same test locations were used each time when these tests were carried out.

3 RESULTS AND DISCUSSION

Results of the tests are shown in Figures 6 to 8. It can be seen from these figures that the damage degree, API and SI increased with an increase in loading level, but had different trends with increased duration of chloride ponding, w/b and type of binder. The effects on the damage degree determined from the UPV values and the Autoclam permeation indices (API and SI) of the beams with increasing load level are summarised in Table 3. Although the application of top up loads resulted in an increase of the damage degree and the Autoclam indices, these are ignored in the following discussion.

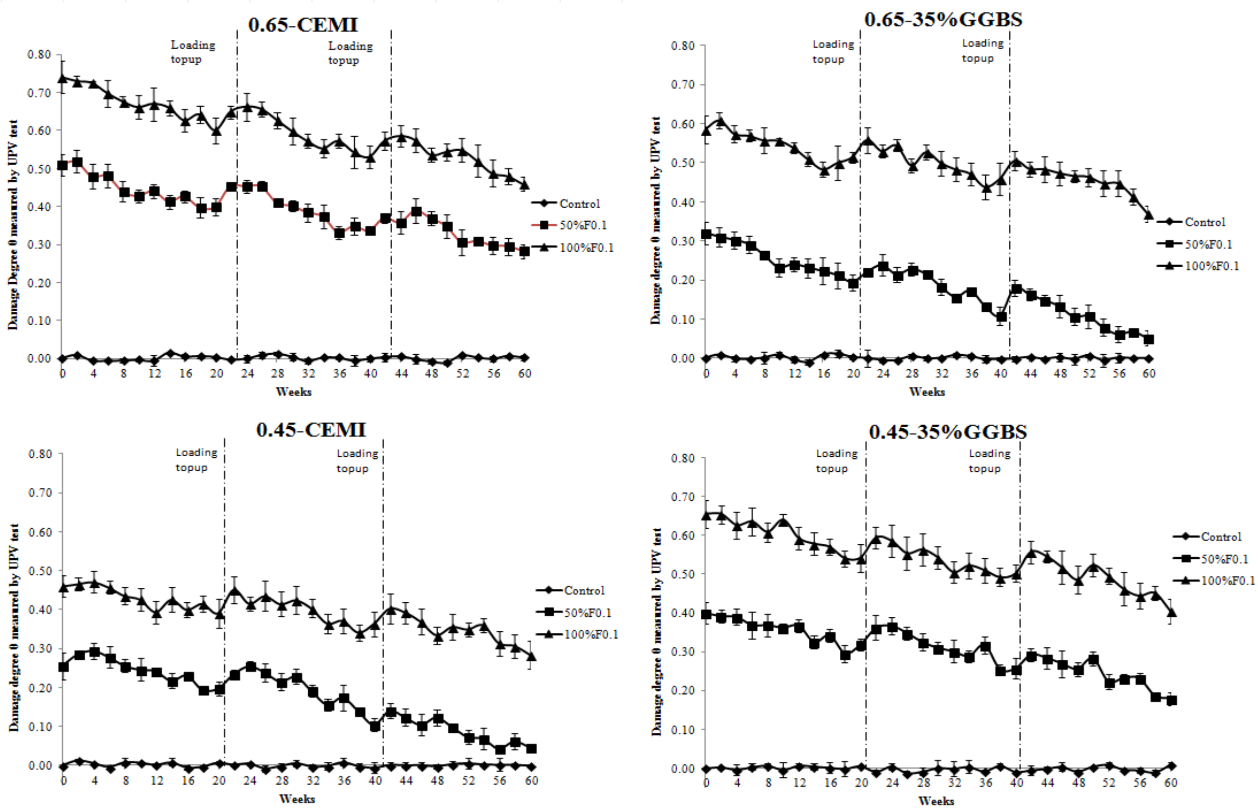

*Figure 6. Damage degree θ of all beams measure*d by UPV test

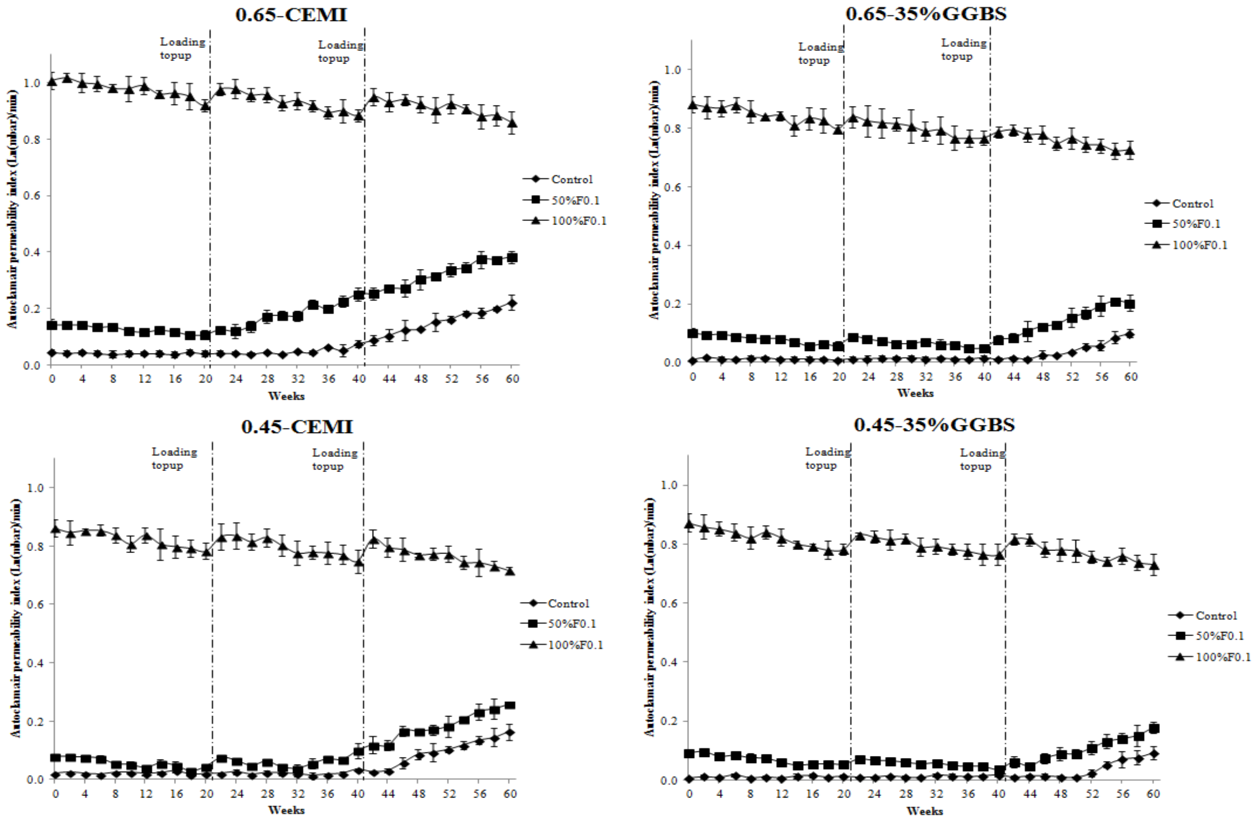

Figure 7. Autoclam air permeability indices of all beams

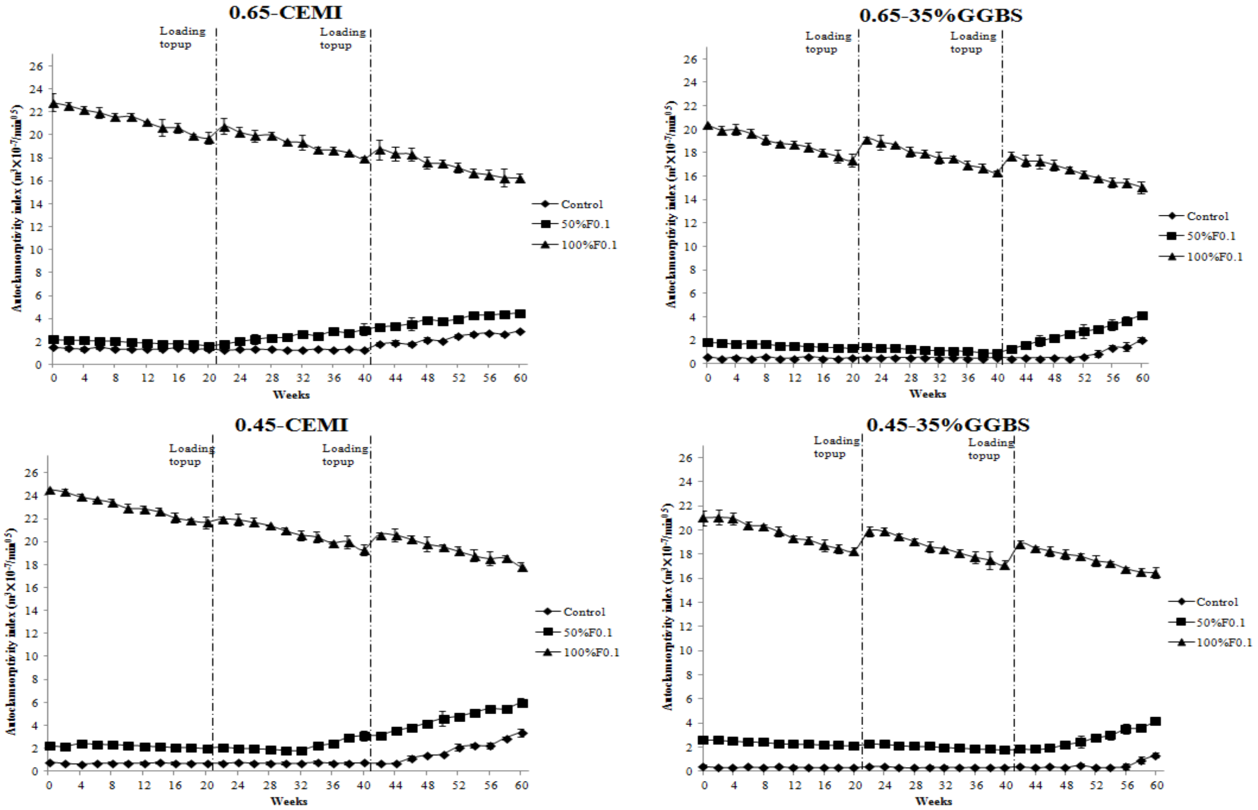

Figure 8 Autoclam sorptivity indices of all beams

Table 3. Influence of duration of ponding, effect of w/b and type of binder on damage degree and Autoclam indices of beams at different load levels

Loading Level	Change in damage degree from UPV			Change in Autoclam indices		
	Effect of duration of ponding	Effect of w/b	Effect of 35%GGBS	Effect of duration of ponding	Effect of w/b	Effect of 35%GGBS
No loading	Remained constant	No effect	No noticeable effect	Remained constant initially, then increased continuously	Both API and SI started increasing at an early period	Both API and SI started increasing at a later period
50% $F_{0.1}$	Decreased continuously	Higher at higher w/b	Increase at 0.45 w/b, but decrease at 0.65 w/b	Slightly decreased initially, then increased continuously	Same as above	Same as above
100% $F_{0.1}$	Same as above	Same as above	Same as above	Decreased continuously	No noticeable effect	No effect

Although the trends in Figure 6 for the damage degree with increased test duration and load level are similar for both w/b and type of cement, there is a different trend in Figures 7 and 8 for the Autoclam permeation indices. Here, similar effects with increased test duration were obtained for no loading and 50% loading conditions, but a totally different trend is seen for the 100% loading condition. For both no loading and 50% loading conditions, the initial variations in API and SI for different mixes are small and this can be attributed to the influence of high level of moisture content in concretes (Basheer et al., 2001). The measurement of relative humidity (RH) before conducting Autoclam tests indicated that the surface RH on all specimens was above 82%, which would suggest that the RH inside the concrete might have been even higher. As reported by Basheer et al. (2001), the air permeability and sorptivity of 0.45 w/c and 0.65 w/c concretes cannot be differentiated if the internal RH is greater than 80%. Due to the particular test regime used in this research, it has not been possible to eliminate the effect of RH on both air permeability and sorptivity fully. Nevertheless, the data in Figures 7 and 8 could be used to discuss the effects of loading and corrosion induced microcracking on both the air permeability and sorptivity.

No loading specimens: From Figures 6, it can be seen that the damage degree measured by UPV test did not change with the increased duration of chloride ponding, but the Autoclam indices of beams (Figures 7 and 8) increased continuously after a certain duration of exposure. The effect of an decrease in w/b was to increase the time at which permeation indices increased. Similarly, with the use of 35% GGBS, there was a substantial increase in time before the permeation indices started to increase. Given that these specimens were not subjected to any loading, it can be concluded that any change in permeation indices is due to corrosion induced microcracking. That is, microcracks caused by the corrosion of steel in the beam have no influence on the damage degree obtained by the indirect UPV method, but could increase both the air permeability and the sorptivity, measured with the Autoclam Permeability System. So, by lowering the w/b and incorporating GGBS in concretes, it is possible to reduce corrosion and corrosion induced microcracking.

50% $F_{0.1}$ loading specimens: Both the damage degree and the Autoclam indices decreased initially with time, which could be due to either self-healing of micro-cracks, the modification of cement hydrates due to the penetration of chloride ions through the cracks (Suryavanshi et al., 1995) or increased moisture content due to cracking. After a certain period of exposure, Autoclam permeation indices increased with time, but the damage degree calculated from the UPV decreased continuously. The continued decrease in damage degree is attributed to the increased moisture content of the concretes and/or self healing effect in large cracks (macro-cracks).

Figure 9 illustrates different directions of the different types of micro-cracks in the beams. As shown in this figure, only the cracks that can alter the transmission route of the ultrasonic pulse wave have an effect on the UPV test. However, as shown in Figure 10, cracks in any direction can have an effect on the Autoclam tests. This suggests that Autoclam test is better to detect the microcracks on the surface of concrete than the UPV test.

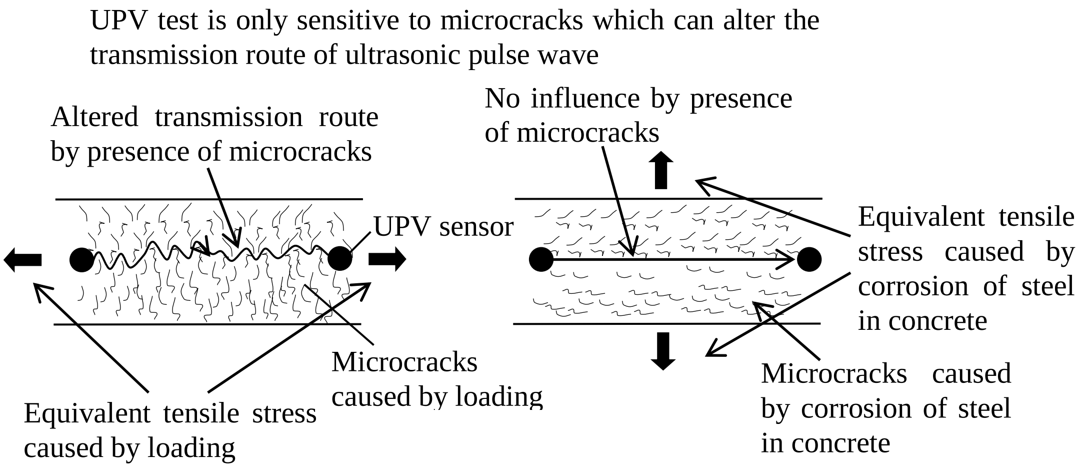

Figure 9. Influence of the orientation of microcracks on UPV test

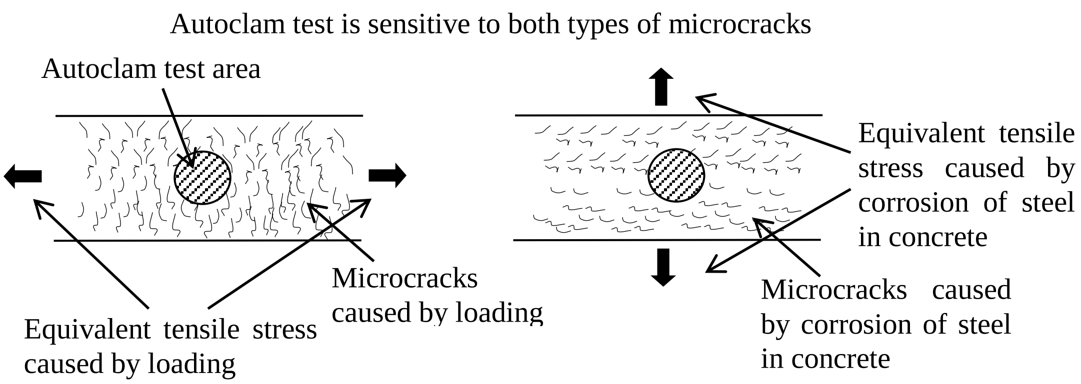

Figure 10. Influence of the orientation of microcracks on Autoclam tests

As shown in Figure 6, the microcracks caused by loading (50%$F_{0.1}$) can increase the damage degree quite significantly compared to no loading condition. However, a corresponding increase in permeation indices was not found. There are two reasons for this disparity in behaviour. It could be argued that there might have been substantial microcracking due to increased loading on the beams. This might increase the UPV and hence the damage degree. However, until the effect of microcracking exceeded the effect of moisture content in concrete, permeation measurements using the Autoclam might not have been influenced. Nevertheless, it can be seen that the time at which the permeation indices started to increase with increased duration of chloride ponding was earlier for 50% $F_{0.1}$ compared to the no loading condition. Therefore, the combined effects of loading and microcracking caused by corrosion could be detected with the Autoclam permeation tests.

100% $F_{0.1}$ loading condition: Both the damage degree and the Autoclam indices decreased continuously with time, as shown in Figures 6-8, but compared to other two loading conditions, there was a substantial increase in both the damage degree and the Autoclam permeation indices. It can be assumed that 100% $F_{0.1}$ loading might have resulted in substantial cracking (both micro and macro sized) of concrete. When these cracks are large in size and volume, it is possible that any damage caused by corrosion is not identified by both the UPV test and the Autoclam tests. Concretes with **macro**-cracks (high load level) can retain large quantities of water and the evaporation rate can be comparatively lower than concretes with **micro**-cracks or no cracks. As a result, there could be an improved self healing effect in their microstructure. Therefore, the decrease in both the damage degree and Autoclam indices could be attributed to a combination of increased moisture content and self healing effects/chemical modifications of the microstructure of concrete.

As summarised in Figure 11, cracks developed on the surfaces of the beams at different exposure time are different, and the related effects on damage degree and Autoclam indices are different.

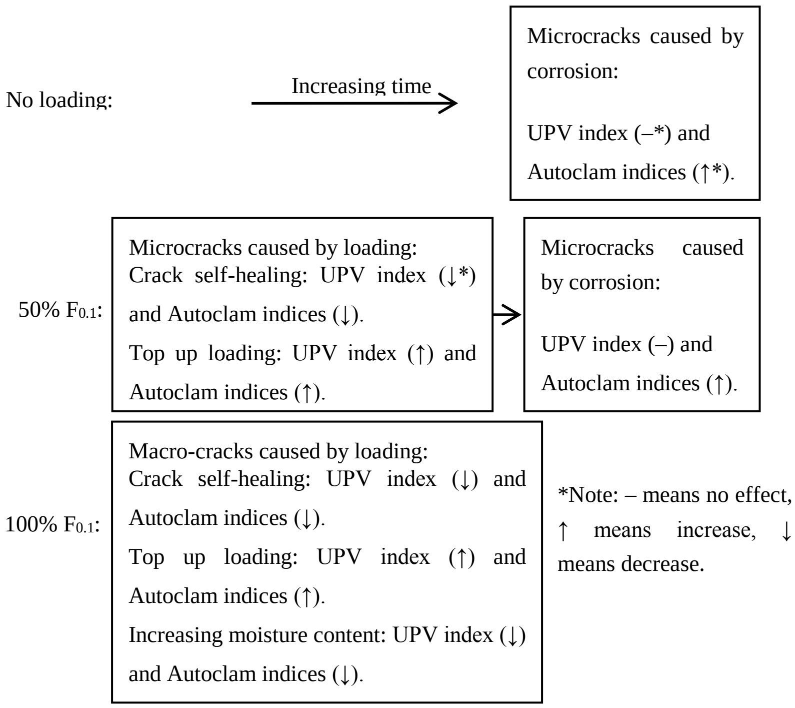

Figure 11. Effects of different types of cracks on UPV test and Autoclam tests with increasing time

4 CONCLUSIONS

By comparison of the results of the two different methods for detecting and monitoring the effect of loading and corrosion induced micro-cracking of concrete, the following conclusions have been made:

1) The indirect method using the UPV test was not able to detect the effects of micro-cracks in concrete caused by the corrosion of the steel. However, it could detect the effect of structural cracks caused by loading.

2) Autoclam permeation tests (air permeability and sorptivity) were sensitive to cracking caused by both structural loading and the corrosion of steel in concrete.

3) The influence of w/b and type of binder on corrosion-induced cracking could be detected using both the air permeability and sorptivity tests. However, if the structural cracking is extensive, there are limitations for detecting the effect of corrosion-induced cracking on permeation properties.

5 REFERENCES

Basheer, P.A.M., Nolan, E. and Long, A.E. 2001, Near surface moisture gradients and in-situ permeation tests, Construction and Building Materials, 15 (2-3), pp 105-114.

British Standards Institution 2011, BS EN 197-1:2011, Cement Part 1: Composition, specifications and conformity criteria for common cements.

British Standards Institution 2004, BS EN 12504-4:2004, Testing concrete - Part 4: Determination of ultrasonic pulse velocity, .

British Standards Institution 1992, BS 6699:1992 Specification for ground granulated blastfurnace slag for use with Portland cement.

British Standards Institution 1989, BS 1881-125:1986 Testing concrete — Part 125: Methods for mixing and sampling fresh concrete in the laboratory.

Jacobsen, S., Marchand, J. & Boisvert, L. 1996, Effect of cracking and healing on chloride transport in OPC concrete, Cement and Concrete Research, vol. 26, no. 6, pp. 869-881.

Wang, J., Basheer, P.A.M., Nanukuttan, S.V. and Bai, Y. 2013a, Influence of microcracking on water transport into reinforced concrete beam under sustained bending. Water Transport in Cementitious Materials. November 3-6, Guildford, UK.

Wang, J., Basheer, P.A.M., Nanukuttan, S.V. and Bai, Y. 2013b, Influence of short-time and sustained compressive loading on chloride migration into concrete. Cement and Concrete Science Conference 2013, September 2-3, Portsmouth, United Kingdom.

Suryavanshi, A.K., Scantlebury, J.D. and Lyon, S.B. 1995, Pore size distribution of OPC & SRPC mortars in presence of chlorides, Cement and Concrete Research, vol. 25, no. 5, pp. 980-988.

Wang, H., Lu, C., Jin, W. and Bai, Y. 2011, Effect of External Loads on the Chloride Transport in Concrete, Journal of Materials in Civil Engineering, vol. 23, no. 7, pp. 1043-1049.